Supporting Information

Tough and Sustainable Solid-Solid Phase Change Materials Achieved via Reversible Crosslinking for Thermal Management

Fubin Luo[1,a], Yaofei Xu[1, a], Dongliang Wang [b], Lebin Zhan [a], Yixin Feng [b], Bili Lin [a], Chunrui Zhai [a], Hongzhou Li [a]*

[a]*Engineering Research Center of polymer Green Recycling of Ministry of Education, College of Environmental and Resource Sciences, Fujian Normal University Fuzhou 350007, People's Republic of China*

[b]*Fujian Key Laboratory of Pollution Control & Resource Reuse, College of Environmental and Resource Sciences, Fujian Normal University, Fuzhou 350007, Fujian Province, People's Republic of China*

* Corresponding author, E-mail address: luofubin@fjnu.edu.cn;

[1] F, L and Y, X contributed equally in this work;

1. Experimental section

Materials

PEG (*Mn*=4000), Pyromellitic dianhydride (PMDA), and 2, 4, 6-Tris (dimethylaminomethyl) phenol (DMP-30, 95%) were provided by Shanghai Macklin ESO chemical Co., Ltd. (Shanghai, China). EP (bisphenol, E51) is provided by Nan Ya Epoxy Resin (Kunshan) Co. Ltd. Hydroxy silicone oil (Mn=2000) was purchased from Silicone Oil House (Shenzhen) Chemical Products Centre (Shenzhen, China). Boron nitride (BN, 50 μm) was purchased from Anhui Zhong Hang Nano Technology Development Co., Ltd. (Anhui, China). γ - (2, 3-epoxypropoxy) propytrimethosysilane (KH-560) was provided by Kangjin New Material Technology Co. Ltd. (Guangdong, China).

Synthesis

Preparation of PEG/PMDA: The preparation procedure for PEG/PMDA resembles our previous work. As previously reported[1], the dried PEG is positioned in a two-necked flask and heated to 120 ℃ until it fully melts. Subsequently, the appropriate mass of PMDA, calculated based on a mass ratio of PEG to PMDA of 10:1, is introduced and allowed to react for 2 hours. Afterward, the mixture is poured into a PTFE mold to cool.

Preparation of epoxy terminated silicone *EPTS*: In a flask, 70 grams of hydroxyl silicone oil (with a molecular weight of 2000) and 11 grams of KH-560 were mixed and subjected to a reaction at 90 ℃ for a duration of 6 hours. Following this, a reduced-pressure distillation apparatus was attached to eliminate the volatile small molecules,

resulting in the production of EPTS.

Preparation of SSPCMs: The prepared EPTS was blended with EP in the appropriate ratio. Next, PEG/PMDA were melted and mixed with the EPTS/EP blend at a ratio where the carboxylic acid groups to epoxy groups was 1:1. A specific amount of the catalyst, 2, 4, 6-Tris (dimethylaminomethyl) phenol (DMP-30, 95%), was then added and stirred thoroughly until a homogeneous mixture was achieved. The ratio of EPTS to EP was displayed in Table S1. The sample was subsequently cured at 150 ℃ for 5 hours and named PEG/PMDA/EPTS/EP. To create thermally conductive phase change composites, boron nitride (BN) was incorporated, and the final composite was designated as PEG/PMDA/EPTS/EP/BNXX, where "XX" indicates the mass fraction of BN (as detailed in Table S3).

Characterization

The microstructure of the composites was determined by using Hitachi Regulus 8100 (Japan) microscope operating under vacuum with a 10 kV voltage. DSC curves were registered on a differential scanning calorimeter (TA Q20) at a selected scanning rate. All the samples were heated from −30 ℃ to 120 ℃ at a scanning rate of 5 ℃ min^{-1} to eliminate the thermal history. XRD graph lines were surveyed with a Bruker D8 diffractometer using filtered Cu-Kα radiation and scanned in the range of 5-60 °at a generator voltage of 40 kV. The temperature-dependent XRD graph lines surveyed with a Bruker D8 diffractometer equipped with a variable-temperature system using filtered Cu-Kα radiation and scanned in the range of 5-60 °at a generator voltage of 40 kV. Thermal decomposition curves were determined from 25 ℃ to 800 ℃ using a

thermogravimetric analyzer (TA Q50) in an inert atmosphere (nitrogen) with a heating rate of 10 ℃ min^{-1}. Thermal conductivities of the composites were measured by a thermal constant analyzer (Hotdisk TPS2500S) and all samples had dimensions of 30 × 30 × 7 mm. The surface morphology of the specimens was observed using a stereomicroscope (AOSVI, T2-3M180). The temperature distribution of the specimen was recorded using a MAG32 infrared thermography camera (Magnity Electronics) for the purpose of visualizing the thermal management of the specimen. The stress–strain property of the specimens were measured by using a universal testing machine. The stress-strain curves were tested by using a dumbbell-type specimen with a width of 4 mm and a thickness of 2 mm. The chemical structure of the materials is confirmed by NMR spectrometer (JEOL JNM-ECZ600R/S1, Japan).

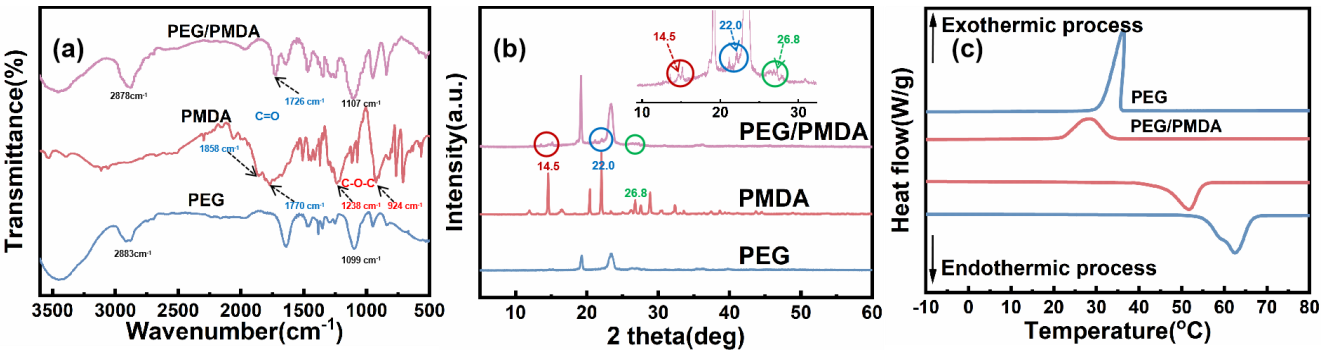

Figure S1 (a) FTIR spectra of PEG, PMDA and PEG/PMDA, (b) XRD patterns of PEG, PMDA and PEG/PMDA, (c) ^{1}H NMR of PEG/PMDA, (d) DSC curves of PEG, PEG/PMDA and PEG/PMDA/EPTS/EP.

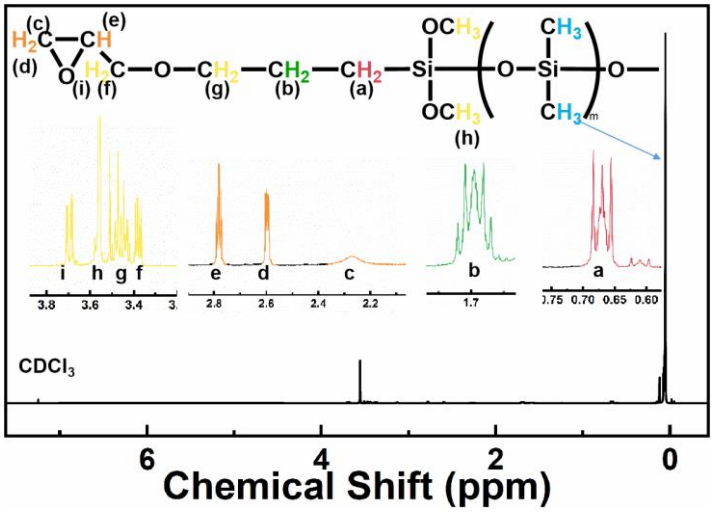

Figure S2 ^{1}H NMR of EPTS.

Table S1 The formula for SSPCMs with varying EPTS content

	PEG/PMDA (mass)	EPTS (mass)	EP (mass)	EPTS:EP
PEG/PMDA/EPTS/EP -1	20	1.67	1.67	1:1
PEG/PMDA/EPTS/EP -2	20	0.9	1.8	1:2
PEG/PMDA/EPTS/EP-4	20	0.47	1.9	1:4
PEG/PMDA/EPTS/EP	20	0.24	1.95	1:8

Table S2 Phase transition enthalpy and temperature of SSPCMs with varying EPTS content

Sample	T_c (°C)	ΔH_c (J/g)	T_m (°C)	ΔH_m (J/g)
PEG	36.28	211.6	62.47	234.4
PEG/PMDA	28.42	135.1	49.57	137.0
PEG/PMDA/EPTS/EP-1	27.42	80.38	48.15	77.87
PEG/PMDA/EPTS/EP-2	24.06	83.15	49.02	78.44
PEG/PMDA/EPTS/EP-4	30.06	88.16	46.35	87.25
PEG/PMDA/EPTS/EP	27.33	92.01	45.20	90.03

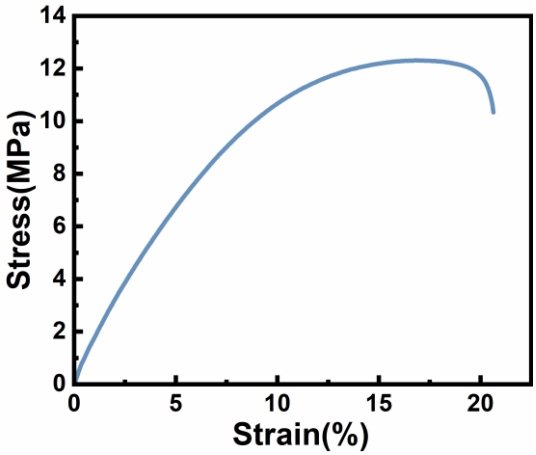

Figure S3 Stress-strain curve of the product obtained from the reaction between EP and PEG/PMDA.

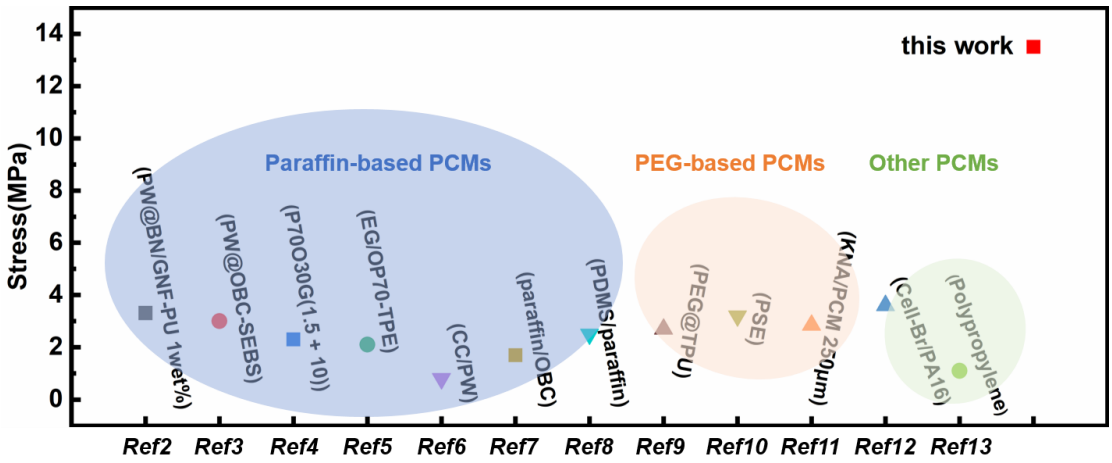

Figure S4 the tensile strength of SSPCMs reported in literatures ([2-13])

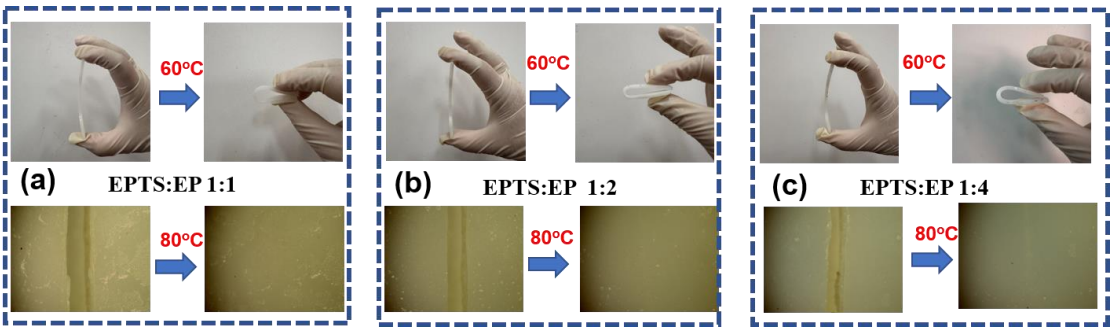

Figure S5 Thermally induced flexibility and self-healing of (a) PEG/PMDA/EPTS/EP-1, (b) PEG/PMDA/EPTS/EP-2 and (c) PEG/PMDA/EPTS/EP-4.

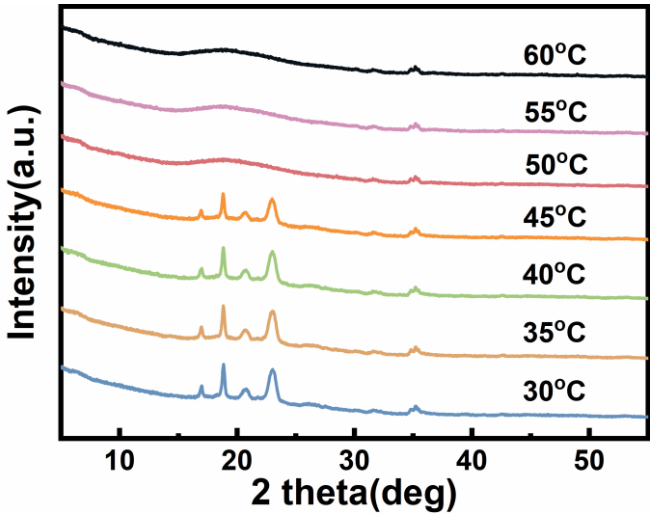

Figure S6 Temperature-dependent XRD spectra of PEG/PMDA/EPTS/EP at different temperatures.

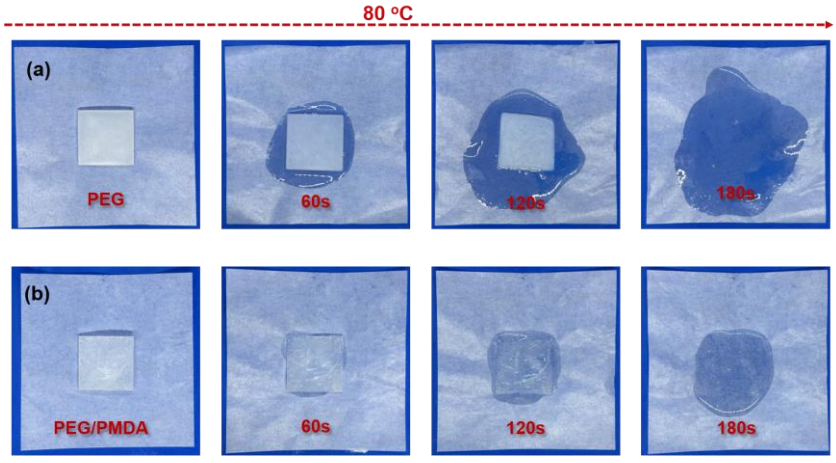

Figure S7 Phase transition of pure PEG and PMDA/PEG upon heating at 80 °C.

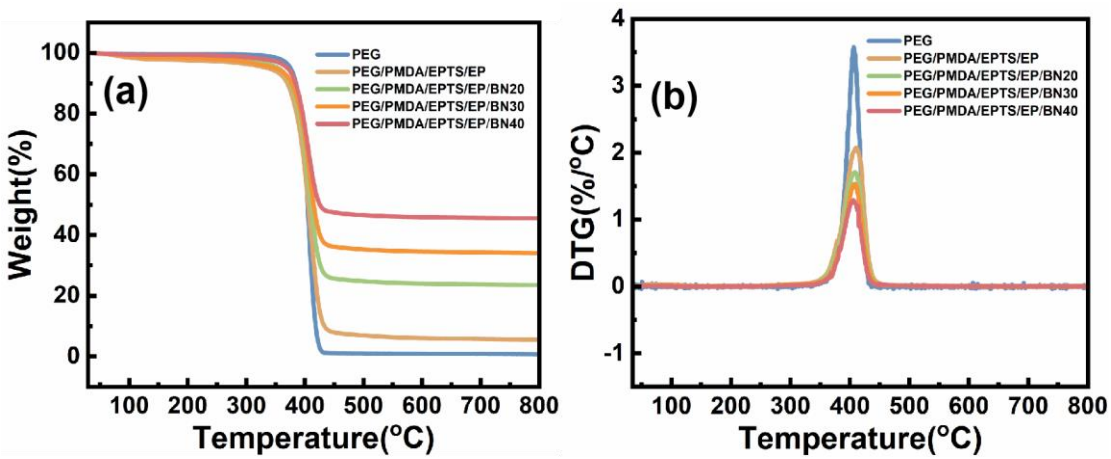

Figure S8 (a) TG and (b) DTG curves of PEG, PEG/PMDA, PEG/PMDA/EPTS/EP and PEG/PMDA/EPTS/EP/BN.

Table S3 PEG/PMDA/EPTS/EP composites filled with BN

	PEG/PMDA (mass)	EPTS (mass)	EP (mass)	BN (%)
PEG/PMDA/EPTS/EP	20	0.24	1.95	0
PEG/PMDA/EPTS/EP/BN20	20	0.24	1.95	20
PEG/PMDA/EPTS/EP/BN30	20	0.24	1.95	30
PEG/PMDA/EPTS/EP/BN40	20	0.24	1.95	40

Table S4 Phase transition enthalpy and temperature of SSPCMs composites

Sample	T_c (°C)	ΔH_c (J/g)	T_m (°C)	ΔH_m (J/g)
PEG/PMDA/EPTS/EP	27.33	92.01	45.20	90.03
PEG/PMDA/EPTS/EP/BN20	28.90	72.90	46.62	71.83
PEG/PMDA/EPTS/EP/BN30	30.06	59.36	45.25	56.36
PEG/PMDA/EPTS/EP/BN40	29.29	44.64	45.20	39.92

[1] Y. Xu, F. Luo, J. Sun, Y. Zou, C. Cao, D. Wang, H. Li, T. Hu, Bio-Based, Recyclable, and Form-Stable Thermally Conductive Phase Change Composite Featuring Thermally Induced Flexibility, ACS Applied Polymer Materials 6(14) (2024) 8671-8678.

[2] N. Sun, Q. Luo, X. Li, Z. Wang, High-Flexible Phase Change Composites with Enhanced Thermal Conductivity for Electronic Thermal Management, ACS Applied Polymer Materials 6(1) (2024) 778-786.

[3] Y. Jing, Z. Zhao, X. Cao, Q. Sun, Y. Yuan, T. Li, Ultraflexible, cost-effective and scalable polymer-based phase change composites via chemical cross-linking for wearable thermal management, Nat Commun 14(1) (2023) 8060.

[4] S. Xue, G. Zhang, Y. Zhang, K. Wu, Q. Fu, Flexible and highly thermally conductive phase change materials with hierarchical dual network for thermal management, Chem. Eng. J. 497 (2024) 154562.

[5] Z. Cai, J. Liu, Y. Zhou, L. Dai, H. Wang, C. Liao, X. Zou, Y. Chen, Y. Xu, Flexible phase change materials with enhanced tensile strength, thermal conductivity and photo-thermal performance, Sol. Energy Mater. Sol. Cells 219 (2021) 110728.

[6] M.M. Umair, Y. Zhang, S. Zhang, X. Jin, B. Tang, A novel flexible phase change composite with electro-driven shape memory, energy conversion/storage and motion sensing properties, Journal of Materials Chemistry A 7(46) (2019) 26385-26392.

[7] X.-d. Qi, Y.-w. Shao, H.-y. Wu, J.-h. Yang, Y. Wang, Flexible phase change composite materials with simultaneous light energy storage and light-actuated shape memory capability, Composites Science and Technology 181 (2019) 107714.

[8] Y. Shi, M. Hu, Y. Xing, Y. Li, Temperature-dependent thermal and mechanical properties of flexible functional PDMS/paraffin composites, Materials & Design 185 (2020) 108219.

[9] Y. Lin, Q. Kang, Y.J. Liu, Y.K. Zhu, P.K. Jiang, Y.W. Mai, X.Y. Huang, Flexible, Highly Thermally Conductive and Electrically Insulating Phase Change Materials for Advanced Thermal Management of 5G Base Stations and Thermoelectric Generators, Nano-Micro Letters 15(1) (2023) 31.

[10] X. Li, W. Yang, C. Li, J. Deng, Q. Huang, W. Jia, Y. Mao, Y. Zou, Y. Wu, J. Tian, G. Zhang, X. Tang, D. Shao, Y. Zhang, S. Zhu, X. Li, Flexible solid-solid phase change material with zero leakage via in-situ preparation for battery thermal management, The Innovation Energy 1(3) (2024) 100034.

[11] J. Lyu, Z. Liu, X. Wu, G. Li, D. Fang, X. Zhang, Nanofibrous Kevlar Aerogel Films and Their Phase-Change Composites for Highly Efficient Infrared Stealth, ACS Nano 13(2) (2019) 2236-2245.

[12] Y. Qian, N. Han, Z. Zhang, R. Cao, L. Tan, W. Li, X. Zhang, Enhanced Thermal-to-Flexible Phase Change Materials Based on Cellulose/Modified Graphene Composites for Thermal Management of Solar Energy, ACS Appl Mater Interfaces 11(49) (2019) 45832-45843.

[13] C. Lin, Y. Yan, Z. Liu, H. Ke, Z. Qiu, R. Hufenus, Flexible phase change filament with ionic liquid core, Journal of Applied Polymer Science 136(32) (2019) 47830.